Fast-forward scaling of atom-molecule conversion in Bose-Einstein condensates

Jing-Jun Zhu [1] and Xi Chen [1,2,*]

[1] *International Center of Quantum Artificial Intelligence for Science and Technology (QuArtist) and Department of Physics, Shanghai University, 200444 Shanghai, China*

[2] *Department of Physical Chemistry, University of the Basque Country UPV/EHU, Apartado 644, 48080 Bilbao, Spain*

(Received 11 December 2020; accepted 19 January 2021; published 4 February 2021)

Robust stimulated Raman exact passages are requisite for controlling nonlinear quantum systems, with wide applications, ranging from ultracold molecules to nonlinear optics to superchemistry. Inspired by shortcuts to adiabaticity, we propose the fast-forward scaling of stimulated Raman adiabatic processes with nonlinearity involved, describing the transfer from an atomic Bose-Einstein condensate to a molecular one by controllable external fields. The fidelity and robustness of atom-molecule conversion are shown to surpass those of conventional adiabatic passages, assisted by the fast-forward driving field. Finally, our results are extended to fractional stimulated Raman adiabatic processes for the coherent superposition of atomic and molecular states.

DOI: 10.1103/PhysRevA.103.023307

I. INTRODUCTION

Over the past few decades, coherent control has been considered a strategic cross-sectional field of research for atomic, molecular, and optical physics and photochemistry, providing a set of quantum mechanics–based methods for the manipulation of populations, typically by laser pulses [1–7]. For example, the coherent control of chemical interactions exemplifies its fascinating applications in chemistry for manipulating and enhancing the product yield [8]. Another intriguing application is so-called superchemistry, in which the coherent Raman transition generates a molecular Bose-Einstein condensate (BEC) from an atomic BEC [9,10]. With the advancement of modern quantum technologies, quantum control has also emerged as an essential physical basis for state preparation and manipulation in quantum information science and quantum sensing [11,12].

In this context, there exist several promising techniques for controlling quantum states coherently, such as adiabatic passages [1,4,6], composite pulses [13,14], optimal control theory [12], and single-shot shaped pulses [15,16]. Along with these techniques, the concept of "shortcuts to adiabaticity" (STA) provides an alternative control paradigm that improves the speed and robustness of the control process [17,18]. In the case of controlled population transfer, methods like counterdiabatic (CD) driving [19–21] (alternatively, the quantum transitionless algorithm [22–24]), invariant-based inverse engineering (IE) [25–27], fast-forward (FF) scaling [28–30] and the dressed state method [31] are capable of speeding up conventional rapid adiabatic passage (RAP) and stimulated Raman adiabatic passage (STIRAP) in two- and three-level quantum systems, respectively. Despite the experimental demonstrations in various quantum platforms with nitrogen-vacancy center spins [32–34], cold atoms [35], and superconducting circuits [36], it is still essential to choose or combine these approaches, depending on the specific systems and objectives of the study, using appropriate features, overlaps, and relations among them [37,38].

Quite naturally, STIRAP and its variants [5,6] have been exploited to study the magneto- and photoassociation of a BEC, by using partially overlapping pulses (pump and Stokes lasers) to produce complete population transfer between two quantum states of an atom or molecule [39–45]. However, the nonlinearity induced from a three-body collision leads to dynamical instability and inefficiency, with the resulting breakdown of adiabaticity [46–48]. In recent years, the technique of STA [49,50], in addition to optimal control [53,54] and adiabatic tracking [51,52], is considered a preferable option to enhance the stability and efficiency of nonlinear STIRAP.

In this article, we explore the FF scaling of atom-molecule conversion in BECs with inherent second-order nonlinearities, by extending the FF method to assist STIRAP [55,56]. Using the dark state in nonlinear Λ-type STIRAP as an ansatz, we construct an FF driving field in the form of couplings between atomic and molecular BECs. We prove that the combination of an FF field and nonlinear STIRAP overcomes the instability and inefficiency of photo- and magnetoassociation of atomic BECs by averting unwanted diabatic transitions. Furthermore, the FF driving field can be similarly designed in nonlinear fractional STIRAP (f-STIRAP), generating the coherent superposition of atomic and molecular BECs. Conceptually, the FF scaling approach in nonlinear STIRAP is different from the CD driving in linear STIRAP, though they have similar forms and presumably similar physical implementations. The instantaneous eigenstates are degenerate and nonorthogonal in nonlinear systems, resulting in an obscure calculation of the CD field. In comparison to the original CD field, the derived FF field is also more general and efficient, with extra control parameters. Moreover, using the FF scaling approach in nonlinear STIRAP, state evolution always takes place along

*xchen@shu.edu.cn

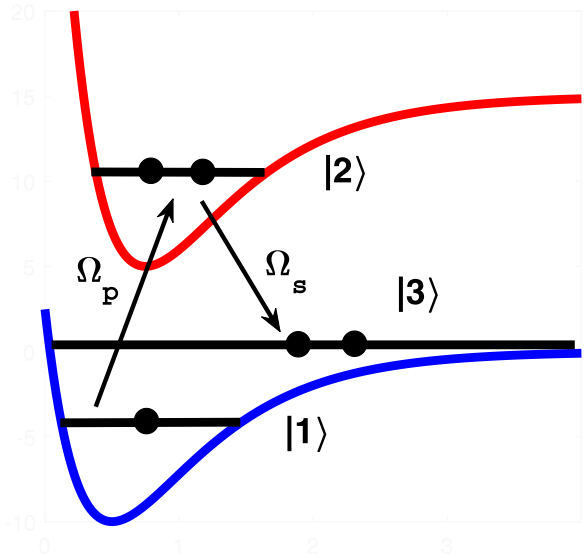

FIG. 1. Schematic of coherent two-color photoassociation of a Bose-Einstein condensate (BEC) in Λ-type STIRAP, where energy levels $|1\rangle$, $|2\rangle$, and $|3\rangle$ present the electronic states for the atomic BEC, the excited molecular BEC, and the stable molecular BEC, respectively; Ω_p and Ω_s are Rabi frequencies for free-bound and bound-bound transitions.

the dark state, leaving the excited states unpopulated. This provides an advantage over the IE method [49], where irreversible losses are inevitable. Finally, we emphasize that our results could be applicable to other nonlinear systems, e.g., nonlinear optics and BECs in an accelerated optical lattice in the presence of third-order Kerr-type nonlinearities.

In Sec. II, we briefly review the model and Hamiltonian of nonlinear STIRAP and its variants. In Sec. III, we derive the formula for the FF driving field accordingly. In Sec. IV, the stability and efficiency of FF-assisted STIRAP and f-STIRAP are featured. Finally, we draw conclusions in Sec. V.

II. MODEL, HAMILTONIAN, AND ADIABATIC PASSAGE

The Schrödinger equation, describing nonlinear STIRAP for coherent two-color photoassociation of a BEC in the mean-field approximation as shown in Fig. 1, can be expressed as the set of differential equations [49]

$$i\dot{c}_1 = K_1 c_1 + \Omega_p \bar{c}_1 c_2, \tag{1a}$$

$$i\dot{c}_2 = K_2 c_2 + \Delta_p c_2 + \Omega_p c_1^2 + \Omega_s c_3, \tag{1b}$$

$$i\dot{c}_3 = K_3 c_3 + (\Delta_p - \Delta_s) c_3 + \Omega_s c_2, \tag{1c}$$

where $\Omega_{p,s} \equiv \Omega_{p,s}(t)$ are the time-dependent Rabi frequencies of the pump and Stokes fields for free-bound and bound-bound transitions, respectively, $\Delta_{p,s}$ represent the corresponding detunings, and c_j is the amplitude in state $|j\rangle$. Here an overdot represents the derivative with respect to time. Typically, the process of photoassociation aims to remove two atoms from state $|1\rangle$ and create a stable molecule in state $|3\rangle$ by using two-laser coupling with a bound-bound molecule in excited state $|2\rangle$. The most intriguing property presented here comes from the second-order nonlinearity, which appears in the form of pump coupling, as well as the third-order Kerr-type nonlinearity, $K_i = \sum_{j=1}^{3} \Lambda_{ij}|c_j|^2$, with Λ_{ij} being some system-dependent constants and populations $|c_j|^2$. In the context of atom-molecular conversion in BECs, the extra c_1 and $\bar{c}_1$ terms appearing in front of Ω_p describe the 1:2 resonance between the ground atomic state and the excited molecular states. The total population is conserved and is normalized as $|c_1|^2 + 2(|c_2|^2 + |c_3|^2) = 1$. Here we write Hamiltonian (1) after performing a change of variable, $c_{2,3} \mapsto c_{2,3}/\sqrt{2}$, yielding the usual normalization, $|c_1|^2 + |c_2|^2 + |c_3|^2 = 1$, for convenience.

Since the resonance-locking condition, $\Delta_p = 2K_1 - K_2$ and $\Delta_s = K_3 - K_2$, compensates Kerr nonlinear terms with detunings [49], we simplify the previous Hamiltonian [see Eq. (1)] within the on-resonance condition as

$$i\dot{c}_1 = \Omega_p \bar{c}_1 c_2, \tag{2a}$$

$$i\dot{c}_2 = \Omega_p c_1^2 + \Omega_s c_3, \tag{2b}$$

$$i\dot{c}_3 = \Omega_s c_2, \tag{2c}$$

where the second-order nonlinearities are still involved, which may lead to dynamical instability [49,50]. In principle, there may exist more nonorthorgonal eigenstates than the dimension of the Hilbert space in nonlinear systems [47]. Nevertheless, in analogy to its linear counterpart [1,6], the nonlinear Λ-type STIRAP still supports a dark state (or so-called coherent population trapping state) with zero eigenvalue [40,44] which is decoupled from the excited state. Therefore, by setting $c_2^0 \simeq 0$ and using $|c_1^0|^2 + |c_3^0|^2 = 1$, we obtain the instantaneous population,

$$\left|c_1^0\right|^2 = 1 - \left|c_3^0\right|^2 = \frac{2\Omega_s}{\Omega_s + \Omega_e}, \tag{3}$$

from which the dark state, corresponding to the eigenvector $|\Psi_0(t)\rangle = [c_1^0, c_2^0, c_3^0]^T$, is calculated as $|\Psi_0(t)\rangle = \mathcal{N}(\Omega_s|1\rangle - c_1^0\Omega_p|3\rangle)$, with $\Omega_e = (\Omega_s^2 + 4\Omega_p^2)^{1/2}$ and $\mathcal{N}$ being the normalization constant. As used in conventional linear STIRAP [1,6], the dark state is further reformulated into

$$|\Psi_0(t)\rangle = \cos\Theta(t)|1\rangle - \sin\Theta(t)|3\rangle, \tag{4}$$

with the mixing angle

$$\Theta(t) = \arctan\left(\frac{c_1^0\Omega_p}{\Omega_s}\right) = \frac{\sqrt{2}\Omega_p}{\sqrt{\Omega_s(\Omega_s + \Omega_e)}}. \tag{5}$$

This dark state has already been experimentally verified, e.g., through the superposition state of atomic and molecular BECs [45]. Apart from it, we have the other two eigenstates, $[0, \pm 1/\sqrt{2}, 1/\sqrt{2}]^T$, with the eigenvalues being $\pm\Omega_s/2$. When $\Omega_s/\Omega_p < 1/\sqrt{2}$, two more eigenstates exist $[(1/2 - \Omega_s^2/\Omega_p^2)^{1/2}, \pm 1/\sqrt{2}, \Omega_s/\Omega_p]^T$ which have the eigenvalues $\pm\Omega_p/\sqrt{2}$. Due to the lack of orthorgonality between the dark state and the other eigenstates, the usual adiabatic condition for linear STIRAP does not hold in the nonlinear case. Thus, one can apply linear stability analysis only around the fixed stable point [43], which corresponds to the dark state, for calculating three orthogonal eigenstates, $w_0 = \mathcal{N}_0[-\Omega_s/2, 0, c_1^0\Omega_p]^T$ and $w_\pm = \mathcal{N}_\pm[c_1^0\Omega_p, \epsilon_\pm, \Omega_s]^T$. The eigenvalues corresponding to $w_{0,\pm}$ are $\epsilon_0 = 0$ and $\epsilon_\pm = \pm\sqrt{\Omega_s\Omega_e}$, respectively. $\mathcal{N}_{0,\pm}$ are the normalization constants.

Accordingly, the adiabatic condition, suitable for nonlinear STIRAP, is derived as [43]

$$A_{\rm nl} \approx \left(\frac{\mathcal{N}_+}{w_+} + \frac{\mathcal{N}_-}{w_-}\right)^{1/2} \left(\frac{\dot{\Omega}_p\Omega_s - \dot{\Omega}_s\Omega_p}{\Omega_s + \Omega_e}\right) \ll 1. \quad (6)$$

It is straightforward to observe, from the adiabatic approximation in Eq. (6), that the pump and Stokes Gaussian pulses [1,6], chosen as

$$\Omega_p(t) = \Omega_0 e^{-(t-\tau)^2/T^2}, \quad (7a)$$

$$\Omega_s(t) = \Omega_0 e^{-(t+\tau)^2/T^2}, \quad (7b)$$

transfer the population from state $|1\rangle$ at initial time $t = t_i$ to $|3\rangle$ at final time $t = t_f$ along the dark state, (4). Note that τ, T, and Ω_0 represent the center, width, and amplitude of the Gaussian pulses, respectively. A more general case would be a combination of one pump and two Stokes Gaussian pulses [57],

$$\Omega_p(t) = \Omega_0 \sin\beta e^{-(t-\tau)^2/T^2}, \quad (8a)$$

$$\Omega_s(t) = \Omega_0 e^{-(t+\tau)^2/T^2} + \Omega_0 \cos\beta e^{-(t-\tau)^2/T^2}, \quad (8b)$$

which asymptotically become

$$0 \overset{t=-\infty}{\longleftarrow} \frac{\Omega_p(t)}{\Omega_s(t)} \overset{t=+\infty}{\longrightarrow} \tan\beta. \quad (9)$$

$\Omega_p(t)$ and $\Omega_s(t)$ create the coherent superposition of $|1\rangle$ and $|3\rangle$ adiabatically by using the dark state. The constant, β, can be determined by the final target state through the combination of Eqs. (5) and (9). Especially for nonlinear f-STIRAP [58], one has to set $\beta = \arctan\sqrt{2}$ when the conditions $\Theta(t_f) = \pi/4$ and $c_1^0(t_f) = 1/\sqrt{2}$ are stipulated to guarantee the state to be a superposition of $|1\rangle$ and $|3\rangle$ with equal amplitudes. Generally it takes a long time to evolve the system when the adiabatic condition, (6), is satisfied, thus spoiling the state by the decoherent effect or repeating the operation at a higher energy cost. In what follows, we develop the FF scaling approach to speed up nonlinear STIRAP and f-STIRAP, thus circumventing such difficulties.

III. FAST-FORWARD SCALING APPROACH

In this section, we generalize the FF scaling approach, with the motivation to accelerate nonlinear STIRAP or f-STIRAP, subjected to a slow variation of pulses. Inspired by the fundamental work of Masuda and Nakamura [28], the FF field for accelerating adiabatic processes has been carried out for several examples like the discrete multilevel quantum system [55,56] and the nonlinear Gross-Pitaevskii equation or the corresponding Schrödinger equation [59,60]. In order to recapitulate the FF scaling for our proposal, we choose the dark state, (4), as an ansatz,

$$|\Psi_{\rm FF}(t)\rangle = \cos[\Theta(R(t))]e^{if_1(t)}|1\rangle - \sin[\Theta(R(t))]e^{if_3(t)}|3\rangle, \quad (10)$$

with $R(t)$ being the "magnification factor" for the rescaled time. The phase factors $f_{1,3}(t)$ are introduced to satisfy the time-dependent Schrödinger equation, $i\partial_t|\Psi_{FF}(t)\rangle = H_{FF}(t)|\Psi_{FF}(t)\rangle$, which becomes

$$i\dot{c}_1 = \Omega_p^{FF}\bar{c}_1c_2 + \Omega_c^{FF}c_3, \quad (11a)$$

$$i\dot{c}_2 = \Omega_p^{FF}c_1^2 + \Omega_s^{FF}c_3, \quad (11b)$$

$$i\dot{c}_3 = \Omega_c^{*FF}c_1 + \Omega_s^{FF}c_2, \quad (11c)$$

with the modified Rabi frequencies of the pump, the Stokes, and an additional FF field being $\Omega_p^{FF} \equiv \Omega_p^{FF}(t)$, $\Omega_s^{FF} \equiv \Omega_s^{FF}(t)$, and $\Omega_c^{FF} \equiv \Omega_c^{FF}(t)$, respectively. Here the boundary conditions $f_{1,3}(t_i) = f_{1,3}(t_f) = 0$ are required to connect to the corresponding adiabatic reference. By inserting this ansatz, (10), into the dynamical equation, we have the following equations:

$$\frac{\Omega_p^{FF}(t)}{\Omega_s^{FF}(t)} = \frac{\sin[\Theta(R(t))]}{\cos^2[\Theta(R(t))]}e^{i[\Delta f(t) - f_1(t)]}, \quad (12)$$

$$\frac{d\Delta f(t)}{dt} = \left\{\frac{2\cos[2\Theta(R(t))]}{\sin[2\Theta(R(t))]}\right\}{\rm Re}\left[\Omega_c^{FF}e^{i\Delta f(t)}\right], \quad (13)$$

$$\frac{\partial\Theta}{\partial R}\frac{\partial R}{\partial t} = {\rm Im}[\Omega_c^{FF}e^{i\Delta f(t)}]. \quad (14)$$

The Rabi frequencies in the FF scaling approach are finally obtained as

$$\frac{\Omega_p^{FF}(t)}{\Omega_s^{FF}(t)} = \frac{\Omega_p(R(t))}{\Omega_s(R(t))}e^{i[\Delta f(t) - f_1(t)]}, \quad (15)$$

$$\Omega_c^{FF}(t) = e^{-i\Delta f(t)}\left\{\frac{\sin[2\Theta(R(t))]}{2\cos[2\Theta(R(t))]}\frac{d\Delta f(t)}{dt} + i\frac{\partial\Theta}{\partial R}\frac{\partial R}{\partial t}\right\}, \quad (16)$$

with $\Delta f(t) = f_3(t) - f_1(t)$. When $f_{1,3}(t) = 0$ is further assumed, the Rabi frequencies can thus be simplified as

$$\frac{\Omega_p^{FF}(t)}{\Omega_s^{FF}(t)} = \frac{\Omega_p(R(t))}{\Omega_s(R(t))}, \quad (17)$$

$$\Omega_c^{FF}(t) = i\frac{\partial\Theta}{\partial R}\frac{\partial R}{\partial t}. \quad (18)$$

Obviously, the additional FF driving field $\Omega_c^{FF}(t)$ is dependent on the magnification factor and essential for the acceleration of adiabatic passages. The pump and Stokes fields, after FF scaling, constitute the same ratio but with the rescaled time. For $R(t) = \eta t$, when the rate of change in $R(t)$ is small, i.e., $\eta \ll 1$, the adiabatic process is recovered The FF field vanishes in this limit, i.e., $\Omega_c^{FF}(t) \simeq 0$. In the case of $R(t) = t$, the FF driving field can be written as $\Omega_c^{FF}(t) = i\dot{\Theta}$, which is similar to the CD driving in linear STIRAP [23]. However, the mixing angle is associated with the c_1^0 in Eq. (5), which results in a different auxiliary interaction between $|1\rangle$ and $|2\rangle$, distinguishing it from its linear counterpart.

It is important to note that, even though the similarities are predominant between the FF scaling, presented here, and other traditional STA methods like CD driving and IE methods, the differences between them are also significant. Though the additional couplings between $|1\rangle$ and $|3\rangle$ are required for both the FF scaling and the CD driving methods, the FF scaling approach is more general in the sense that when $f_{13}(t) \neq 0$, the FF field has both real and imaginary parts with a pulse area larger than π [55]. Most importantly, the FF scaling approach is fundamentally different from CD driving.

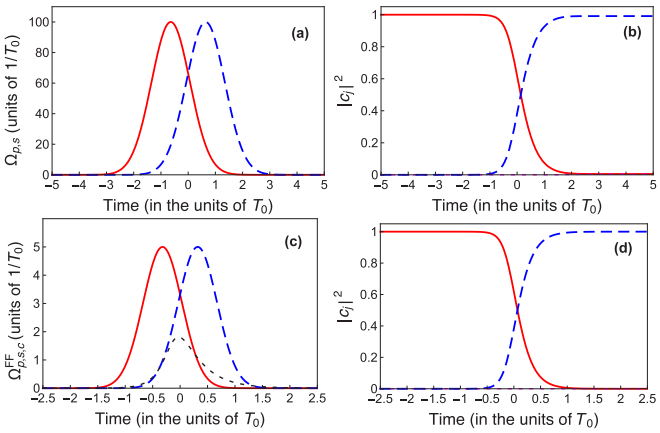

FIG. 2. Nonlinear STIRAP (a) for state transfer (b) from an atomic BEC to a molecular BEC, where Ω_s (solid red lines) and Ω_p (dashed blue lines) sequences are Gaussian type with amplitude $\Omega_0 = 100$ (in units of $1/T_0$), $\tau = 0.64T$, $T = 1$ (in units of T_0), and $T_0 = 3.1 \times 10^{-5}$ s. The final population $|c_3|^2 = 0.9914$ is achieved in total time $10T$. For comparison, FF-assisted STIRAP (c) for state transfer (d) is also presented, where $\Omega_s^{\rm FF}$ (solid red lines) and $\Omega_p^{\rm FF}$ (dashed blue lines) with $\Omega_0 = 5$ and other parameters are the same. Assisted by the FF driving field $\Omega_c^{\rm FF}$ (dotted black lines), the final population $|c_3|^2 = 0.9999$ is achieved with total time $5T$.

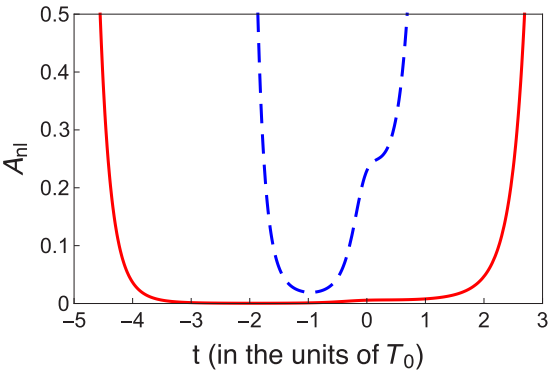

FIG. 3. The parameter $A_{\rm nl}$ is depicted to quantify the adiabatic condition, (6), where the parameters are used for nonlinear STIRAP (solid red line) and FF-assisted STIRAP (dashed blue line) in Fig. 2.

In order to obtain the CD term, one has to calculate the nonadiabatic contribution after diagonalizing the Hamiltonian, which is rather straighforward to calculate, as the eigenspectrum is known in linear STIRAP. On the contrary, in nonlinear STIRAP, we cannot use the eigenstates and their orthogonality to obtain the CD driving directly. Instead, we assume the dark state as an ansatz for constructing the FF driving field, such that the state transfer is always along the dark state. This also provides a significant advantage over the IE method used in Ref. [49], in which the intermediate state $|2\rangle$ is populated, thus leading to inevitable losses. Moreover, various functions of $R(t)$ can be further adopted for accelerating the adiabatic passage, which provides more flexibility as well [59,60]. By selecting the magnification factor $R(t)$ for the rescaled time, the FF scaling is closely connected with the time-rescaled method recently proposed in [61]. However, we should point out that the time-rescaled dynamics, driven by the modified fields, (17), works perfectly only when the original protocol is adiabatic, since the adiabatic condition cannot be improved without the auxiliary coupling [see Eq. (18)].

IV. EFFICIENCY AND STABILITY

We first check the conventional nonlinear STIRAP in the aforementioned Λ-type nonlinear system. By using Gaussian shapes of the pump and Stokes fields [see Eq. (7)], the state can be adiabatically transferred from an atomic BEC at initial time $t_i = -5T$ to a molecular one at $t_f = 5T$, as shown in Figs. 2(a) and 2(b), where $\Omega_0 = 100$ (in units of $1/T_0$), $\tau = 0.64T$, and $T = 1$ (in units of T_0). Normally, $T_0 = 3.1 \times 10^{-5}$ s can be chosen in the practical experiment [39], corresponding to $\Omega_0 = 3.226$ MHz. The final population $|c_3(t_f)|^2 = 0.9914$ is achieved without exciting state $|2\rangle$ when the total time is $10T$ with the fixed $\Omega_0 = 100$. Remarkably, the modified pump and Stokes fields and FF driving field are designed to accelerate nonlinear STIRAP, as shown in Figs. 2(c) and 2(d), where $\Omega_0 = 5$, and other parameters are the same as those in Figs. 2(a) and 2(b). By introducing $R(t) = at$, the total evolution time is decreased up to $5T$ with $a = 2$, when assisted by the FF field. From the comparison in Fig. 2, we demonstrate that the assisted FF driving field really speeds up the original nonlinear STIRAP, by following the dark state, as seen in population evolution. The final population reaches $|c_3|^2 = 0.9999$ in Fig. 2(d), even when the parameters do not fulfill the adiabatic condition, (6). In order to quantify the acceleration, we calculate the adiabatic condition, (6) (see Fig. 3), where $A_{nl} \ll 1$, for the parameters that are used in conventional nonlinear STIRAP. When the transfer time is shortened, the corresponding parameters make A_{nl} significantly large so that the adiabaticity is broken, with lower intensities of the pulses. For simplicity, one can choose $R(t) = t$ while keeping the total time at $10T$. It can still be shown that the auxiliary FF field assists the pump and Stokes fields to achieve the high-fidelity state transfer with $\Omega_0 = 5$. Here, the Gaussian pulses do not fulfill the adiabatic condition and the FF driving field speeds up the nonlinear STIRAP when $R(t) = t$, reducing the system evolution time for small Ω_0. This also clarifies the importance of auxiliary coupling and causes the difference from the time-rescaled method [61], as mentioned before.

Moreover, we select other functions of $R(t)$, demonstrating the diversity. For instance, one option is a trigonometric ansatz [61],

$$R(t) = at - \frac{t_f - t_i}{2\pi a}(a-1)\sin\left[\frac{2\pi a}{t_f - t_i}\left(t - \frac{t_i}{a}\right)\right], \qquad (19)$$

where its inverse function and first derivative satisfy the boundary conditions $R^{-1}(t_i) = t_i/a$, $R^{-1}(t_f) = t_f/a$ and $R'(t_i) = R'(t_f) = 1$. Here the additional conditions on the first derivative imply that the time-rescaled Hamiltonian coincides with the original one at the initial and final times. Figure 4(a) shows the modified pump, Stokes Gaussian pulses for nonlinear STIRAP, and assisted FF driving field. Here we use $a = 2$ to compare the results obtained from $R(t) = 2t$, by keeping the same fidelity at $t = t_f$ asin Fig. 2. We find that the amplitude of Gaussian pulses becomes higher by using the

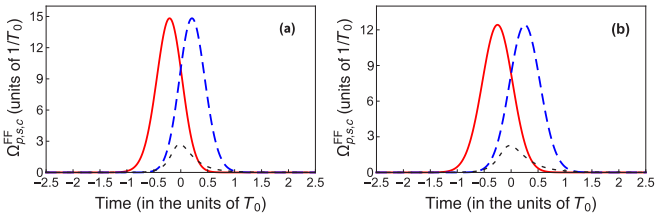

FIG. 4. Using different values of $R(t)$, the modified pump and Stokes Gaussian pulses are presented for nonlinear STIRAP (a, b), together with the assisted FF driving field; $\Omega_s^{\rm FF}$ (solid red lines) $\Omega_p^{\rm FF}$ (dashed blue lines), and $\Omega_c^{\rm FF}$ (dotted black lines). The parameters are the same as in Fig. 2. Here (a) and (b) correspond to the trigonometric and polynomial ansatzes of $R(t)$, respectively.

trigonometric function, while the population dynamics (not shown here) does not change very much. Alternatively, the fourth-degree polynomial, $R(t) = \sum_{i=0}^{3} \eta_j t^i$, can be adopted as well, where the four coefficients η_j are completely solvable by using the aforementioned boundary conditions. We do not write them down explicitly, to avoid the lengthy expression. In this case, the modified pump and Stokes Gaussian pulses are presented in Fig. 4(b), together with the corresponding FF driving field. It is confirmed by the comparison that the proper choice of $R(t)$ helps to decrease the amplitude of pulses.

Next, we also apply the FF driving field for accelerating nonlinear f-STIRAP. In Figs. 5(a) and 5(b) we recover the original adiabatic process to generate the coherent superposition of an atomic BEC and a molecular BEC with equal amplitudes where Gaussian pulses of the pump and Stokes fields are used [see Eq. (8)], with $\Omega_0 = 20$ and $\beta = \sqrt{2}$. Similarly to nonlinear STIRAP, we apply the FF driving field along

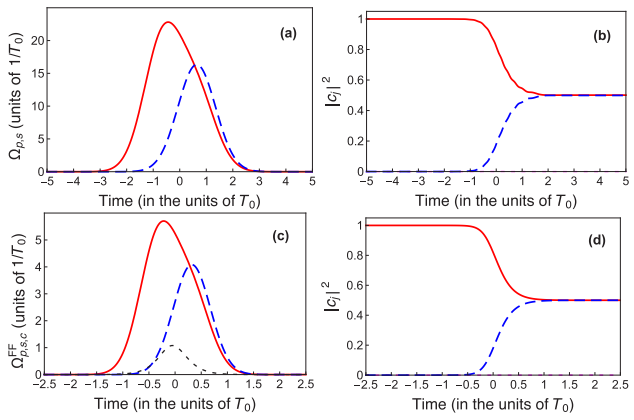

FIG. 5. Nonlinear f-STIRAP (a) for generating the coherent state superposition (b), where Ω_s (solid red lines) and Ω_p (dashed blue lines) sequences are Gaussian type with amplitude $\Omega_0 = 20$ (in units of $1/T_0$), $\tau = 0.64T$, $T = 1$ (in units of T_0), and $T_0 = 3.1 \times 10^{-5}$ s. The superposition of an atomic BEC and a molecular BEC with equal amplitudes is provided with total time $10T$. For comparison, FF-assisted f-STIRAP (c) for generating such a superposition (d) is also presented, where $\Omega_s^{\rm FF}$ (solid red lines) and $\Omega_p^{\rm FF}$ (dashed blue lines) with $\Omega_0 = 5$ and the other parameters are the same. Assisted by the FF driving field $\Omega_c^{\rm FF}$ (dotted black lines), the superposition of atomic and molecular BECs with equal amplitudes is achieved with total time $5T$.

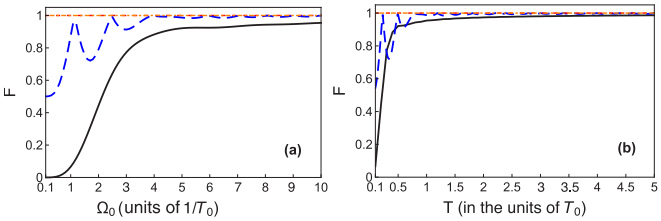

FIG. 6. Fidelity, $F = |\langle\Psi_0(t_f)|\Psi(t_f)\rangle|^2$, versus the amplitude Ω_0 (a) and the width T (b) of Gaussian pulses, where $\Psi_0(t_f)$ is the target state and $|\Psi(t_f)\rangle$ is the final solution of the time-dependent Schrödinger equation. Here the fidelities of nonlinear STIRAP, nonlinear f-STIRAP, and FF-assisted STIRAP, denoted by solid black, dashed blue, and dotted red lines, and that of FF-assisted f-STIRAP (dash-dotted orange line) are undistinguishable. Other parameters are the same as in Figs. 2 and 5.

with the modified pump and Stokes fields to speed up the nonlinear f-STIRAP [see Figs. 5(c) and 5(d)]. Here we choose the rescaling function as $R(t) = 2t$ for simplicity, which can shorten the total evolution time from $10T$ to $5T$, with the low coupling amplitude $\Omega_0 = 5$. With the assisted FF driving field, the state evolution follows exactly the adiabatic reference in Figs. 5(b) and 5(d) to achieve the perfect coherent superposition at the ratio 1:1, but without populating excited state $|2\rangle$. It is evident in Fig. 5 that the FF scaling approach provides the desired state superposition, which can be generalized for other ratios of amplitudes as well by changing the parameter β in Eq. (8) through the mixing angle, (5).

Finally, we address the issue of the efficiency and stability of nonlinear STIRAP and f-STIRAP assisted by the FF driving field. Figure 6(a) demonstrates that the fidelity F depends strongly on the amplitude Ω_0 of STIRAP and f-STIRAP, where the fidelity can be defined as $F = |\langle\Psi_0(t_f)|\Psi(t_f)\rangle|^2$, with $|\Psi_0(t_f)\rangle$ being the target state (the dark state at $t = t_f$) and $|\Psi(t_f)\rangle$ being the final solution of the time-dependent Schrödinger equation. It is clear that the adiabatic passages do not work for small values of Ω_0, due to the breakdown of the adiabatic condition. For instance, when $\Omega_0 = 10$ is chosen, which is much less than $\Omega_0 = 100$, as used in Fig. 2, the fidelity of nonlinear STIRAP is far from unity. Remarkably, the designed FF driving field accelerates the adiabatic passage with perfect fidelity, $F \simeq 1$, for an arbitrary value of Ω_0. In addition, as shown in Fig. 5, $\Omega_0 = 20$ is required for nonlinear f-STIRAP to meet the adiabatic criteria. With the assisted FF driving, perfect population transfer can be achieved when $\Omega_0 = 5$. However, one has to keep in mind that the energetic cost of STA, that is, the physical constraint on the FF driving field sets the limitation to shorten the time, relevant to quantum speed limits [62]. We also confirm that the FF scaling approach improves the stability with respect to the fluctuations in T, as shown in Fig. 6(b). The fidelity decreases dramatically for the adiabatic case when T is shortened. However, ideally, it always remains close to unity, i.e., $F \simeq 1$ regardless of the value chosen for T, when the FF driving field is complemented. Furthermore, the stability with respect to τ, affecting the sequence of Gaussian pulses, is improved by the FF driving field as well. For instance, the fidelities are decreased down to $F = 0.9790$ and 0.9953, respectively, for the original nonlinear STIRAP and f-STIRAP when

$\tau = 0.5T$. However, with the assisted FF field, the fidelities remain $F \simeq 1$ in both protocols, where T is rescaled by the magnification factor $R(t) = 2t$ with the assisted FF field. Moreover, we check that the other protocols for previously mentioned $R(t)$ maintain the same feature of robustness against variation of Ω_0 and T. Actually, the increased robustness makes sense, as the area of the whole pump and Stokes Gaussian pulses is increased by π (for nonlinear STIRAP) and $\pi/2$ (for nonlinear f-STIRAP), which is induced from the FF driving field. Interestingly, we may simplify the STA recipe in this case by using a one-photon 1-3 pulse, instead of the original two-photon transition [23]. However, the resonant pulses, i.e., π (or $\pi/2$) pulses, are sensitive to parameter fluctuation. As far as physical implementations are concerned, the transition induced from the designed FF driving field can be physically implemented by a magnetic dipole transition, if the electric dipole is forbidden. Therefore, the intensity of the magnetic field, which directly couples states $|1\rangle$ and $|3\rangle$, limits the ability to shorten the time infinitely. Upon combination with the laser fields, the FF driving field, connecting levels $|1\rangle$ and $|3\rangle$, should be on resonance with the Raman transition, which could be problematic due to the phase mismatch and can easily be avoided by shaping the pulses through unitary transformations [35].

V. CONCLUSION

In summary, we have worked out the FF scaling of coherent control for atom and molecular BECs, with second-order nonlinearity involved. By using the dark state in a nonlinear Λ-type system, we derive the FF driving field, which, when combined with the modified pump and Stokes fields, can produce high-fidelity state conversion from an atomic BEC to a molecular one beyond the adiabatic regime. Moreover, the result can be directly generalized to nonlinear f-SITRAP for the coherent superposition of an atomic and a molecular BEC. FF-assisted STIRAP and f-STIRAP have a higher tolerance to the fluctuations in various parameters such as the intensity and the width of Gaussian pulses. In addition, the original adiabatic passages are speeded up, but without populating the intermediate excited state, which prevents losses due to inevitable dissipation [44] or the dephasing effect [63].

We must emphasize that the FF scaling approach in nonlinear systems is different from CD driving and the IE method of STA. In a nonlinear system, the eigenstates are generally nonorthogonal and degenerate, which hinders the calculation of CD driving, even though the expression of the FF field is similar. With extra parameters in the phase of the dark state, (4), FF driving provides more flexibility for atom-molecular conversion, with large areas of pulses. We realize that the intermediate state $|2\rangle$ is populated in an alternative IE method [49], in which one of the dynamical modes of the Lewis-Riesenfeld invariant for its linear counterpart is applied [64]. However, the price paid in the FF scaling approach is the supplement of the auxiliary coupling between state $|1\rangle$ and state $|3\rangle$. And the availability of such coupling will set the limitation to shorten the time. Therefore, when it comes to experimental realization, one can pick up the suitable recipes or protocols as discussed above, taking the physical feasibility and limitations into account. Moreover, there are many choices of the magnification factor $R(t)$ for the rescaled time, which give different pulse amplitudes. One can further investigate elsewhere to optimize it with respect to the amplitude of pulses and the robustness against parameter variations, e.g., by using analytical enhanced STA [65] or combining other numerical recipes.

Last but not least, the FF scaling approach is interestingly extended to study fast and robust control of unstable nonlinear systems, such as BECs in optical lattices with third-order Kerr-type nonlinearity [66], other applications of coupled waveguides [67,68], and frequency conversion in nonlinear optics [69], in an analogous fashion.

ACKNOWLEDGMENTS

We thank Koushik Paul for his valuable discussions and comments. We acknowledge support from the NSFC (Grant No. 12075145), the STCSM (Grants No. 2019SHZDZX01-ZX04, No. 18010500400, and No. 18ZR1415500), the Program for Eastern Scholar, Spanish Government Grant No. PGC2018-095113-B-I00 (MCIU/AEI/FEDER, UE), and Basque Government Grant No. IT986-16. X.C. acknowledges the Ramón y Cajal program (Grant No. RYC2017-22482).

[1] K. Bergmann, H. Theuer, and B. Shore, Rev. Mod. Phys. **70**, 1003 (1998).
[2] M. Shapiro and P. Brumer, Adv. Atom. Mol. Opt. Phys. **42**, 287 (2000).
[3] S. Guérin and H. R. Jauslin, Adv. Chem. Phys. **125**, 147 (2003).
[4] P. Král, I. Thanopulos, and M. Shapiro, Rev. Mod. Phys. **79**, 53 (2007).
[5] K. Bergmann, N. V. Vitanov, and B. W. Shore, J. Chem. Phys. **142**, 170901 (2015).
[6] N. V. Vitanov, A. A. Rangelov, B. W. Shore, and K. Bergmann, Rev. Mod. Phys. **89**, 015006 (2017).
[7] B. W. Shore, *Manipulating Quantum Structures Using Laser Pulses* (Cambridge University Press, Cambridge, UK, 2011).
[8] P. Brumer and M. Shapiro, Annu. Rev. Phys. Chem. **43**, 257 (1992).
[9] D. J. Heinzen, R. Wynar, P. D. Drummond, and K. V. Kheruntsyan, Phys. Rev. Lett. **84**, 5029 (2000).
[10] J. J. Hope and M. K. Olsen, Phys. Rev. Lett. **86**, 3220 (2001).
[11] D. D'Alessandro, Introduction to Quantum Control and Dynamics (*Advances in Applied Mathematics*) (Chapman and Hall/CRC, Boca Raton, FL, 2007).
[12] S. J. Glaser, U. Boscain, T. Calarco, Christiane P. Koch, W. Kockenberger, R. Kosloff, I. Kuprov, B. Luy, S. Schirmer, T. Schulte-Herbruggen, D. Sugny, and F. K. Wilhelm, Eur. Phys. J. D **69**, 279 (2015).
[13] M. H. Levitt, Prog. Nucl. Magn. Reson. Spectrosc. **18**, 61 (1986).

[14] B. T. Torosov, S. Guérin, and N. V. Vitanov, Phys. Rev. Lett. **106**, 233001 (2011).
[15] E. Barnes and S. Das Sarma, Phys. Rev. Lett. **109**, 060401 (2012).
[16] D. Daems, A. Ruschhaupt, D. Sugny, and S. Guérin, Phys. Rev. Lett. **111**, 050404 (2013).
[17] D. Guéry-Odelin, A. Ruschhaupt, A. Kiely, E. Torrontegui, S. Martínez-Garaot, and J. G. Muga, Rev. Mod. Phys. **91**, 045001 (2019).
[18] E. Torrontegui, S. Ibánez, S. Martínez-Garaot, M. Modugno, A. del Campo, D. Guéry-Odelin, A. Ruschhaupt, X. Chen, and J. G. Muga, Adv. Atom. Mol. Opt. Phys. **62**, 117 (2013).
[19] R. Unanyan, L. Yatsenko, K. Bergmann, and B. W. Shore, Opt. Commun. **139**, 48 (1997).
[20] M. Demirplak and S. A. Rice, J. Phys. Chem. A **107**, 9937 (2003).
[21] M. Demirplak and S. A. Rice, J. Chem. Phys. **129**, 154111 (2008).
[22] M. V. Berry, J. Phys. A: Math. Theor. **42**, 365303 (2009).
[23] X. Chen, I. Lizuain, A. Ruschhaupt, D. Guéry-Odelin, and J. G. Muga, Phys. Rev. Lett. **105**, 123003 (2010).
[24] Y.-C. Li and X. Chen, Phys. Rev. A **94**, 063411 (2016).
[25] A. Ruschhaupt, X. Chen, D. Alonso, and J. G. Muga, New J. Phys. **14**, 093040 (2012).
[26] X.-J. Lu, X. Chen, A. Ruschhaupt, D. Alonso, S. Guérin, and J. G. Muga, Phys. Rev. A **88**, 033406 (2013).
[27] X. Chen and J. G. Muga, Phys. Rev. A **86**, 033405 (2012).
[28] S. Masuda and K. Nakamura, Proc. R. Soc. A **466**, 1135 (2010).
[29] K. Takahashi, Phys. Rev. A **89**, 042113 (2014).
[30] I. Setiawan, B. Eka Gunara, S. Masuda, and K. Nakamura, Phys. Rev. A **96**, 052106 (2017).
[31] A. Baksic, H. Ribeiro, and A. A. Clerk, Phys. Rev. Lett. **116**, 230503 (2016).
[32] J. Zhang, J. H. Shim, I. Niemeyer, T. Taniguchi, T. Teraji, H. Abe, S. Onoda, T. Yamamoto, T. Ohshima, J. Isoya, and D. Suter, Phys. Rev. Lett. **110**, 240501 (2013).
[33] B. B. Zhou, A. Baksic, H. Riberio, C. G. Yale, F. J. Heremans, P. C. Jerger, A. Auer, G. Burkard, A. A. Clerk, and D. D. Awschalom, Nat. Phys. **13**, 330 (2017).
[34] J. Kölbl, A. Barfuss, M. S. Kasperczyk, L. Thiel, A. A. Clerk, H. Ribeiro, and P. Maletinsky, Phys. Rev. Lett. **122**, 090502 (2019).
[35] Y. Du, Z. Liang, Y. Chao, X. Yue, Q. Lv, W. Huang, X. Chen, H. Yan, and S.-L. Zhu, Nat. Commun. **7**, 12479 (2016).
[36] A. Vepsäläinen, S. Danilin, and G. S. Paraoanu, Sci. Adv. **5**, eaau5999 (2019).
[37] X. Chen, E. Torrontegui, and J. G. Muga, Phys. Rev. A **83**, 062116 (2011).
[38] E. Torrontegui, S. Martínez-Garaot, A. Ruschhaupt, and J. G. Muga, Phys. Rev. A **86**, 013601 (2012).
[39] R. Wynar, R. S. Freeland, D. J. Han, C. Ryu, and D. J. Hainzen, Science **287**, 1016 (2000).
[40] M. Mackie, R. Kowalski, and J. Javanainen, Phys. Rev. Lett. **84**, 3803 (2000).
[41] J. J. Hope, M. K. Olsen, and L. I. Plimak, Phys. Rev. A **63**, 043603 (2001).
[42] P. D. Drummond, K. V. Kheruntsyan, D. J. Heinzen, and R. H. Wynar, Phys. Rev. A **65**, 063619 (2002).
[43] H.-Y. Ling, H. Pu, and B. Seaman, Phys. Rev. Lett. **93**, 250403 (2004).
[44] M. Mackie, K. Härkönen, A. Collin, K.-A. Suominen, and J. Javanainen, Phys. Rev. A **70**, 013614 (2004).
[45] K. Winkler, G. Thalhammer, M. Theis, H. Ritsch, R. Grimm, and J. H. Denschlag, Phys. Rev. Lett. **95**, 063202 (2005).
[46] H. Y. Ling, P. Maenner, W.-P. Zhang, and H. Pu, Phys. Rev. A **75**, 033615 (2007).
[47] J. Liu, B. Wu, and Q. Niu, Phys. Rev. Lett **90**, 170404 (2003).
[48] A. P. Itin and S. Watanabe, Phys. Rev. Lett. **99**, 223903 (2007).
[49] V. Dorier, M. Gevorgyan, A. Ishkhanyan, C. Leroy, H. R. Jauslin, and S. Guérin, Phys. Rev. Lett. **119**, 243902 (2017).
[50] J.-J. Zhu, X. Chen, H. R. Jauslin, and S. Guérin, Phys. Rev. A **102**, 052203 (2020).
[51] S. Guérin, M. Gevorgyan, C. Leroy, H. R. Jauslin, and A. Ishkhanyan, Phys. Rev. A **88**, 063622 (2013).
[52] M. Gevorgyan, S. Guérin, C. Leroy, A. Ishkhanyan, and H. R. Jauslin, Eur. Phys. J. D **70**, 253 (2016).
[53] M. Vatasescu, O. Dulieu, R. Kosloff, and F. Masnou-Seeuws, Phys. Rev. A **63**, 033407 (2001).
[54] X. Chen, Y. Ban, and G. C. Hegerfeldt, Phys. Rev. A **94**, 023624 (2016).
[55] S. Masuda and S. A. Rice, J. Phys. Chem. A **119**, 14, 3479 (2015).
[56] S. Masuda and S. A. Rice, Adv. Chem. Phys **159**, 51 (2016).
[57] N. V. Vitanov, K.-A. Suominen, and B. W. Shore, J. Phys. B **32**, 4535 (1999).
[58] N. Shirkhanghah and M. Saadati-Niari, Revista Mex. Fís. **66**, 344 (2020).
[59] S. Masuda and K. Nakamura, Phys. Rev. A **78**, 062108 (2008).
[60] S. Masuda and K. Nakamura, Phys. Rev. A **84**, 043434 (2011).
[61] B. de Lima Bernardo, Phys. Rev. Res. **2**, 013133 (2020).
[62] O. Abah, R. Puebla, A. Kiely, G. De Chiara, M. Paternostro, and S. Campbell, New J. Phys. **21**, 103048 (2019).
[63] H. Z. Shen, X.-M. Xiu, and X. X. Yi, Phys. Rev. A **87**, 063613 (2013).
[64] A. Benseny, A. Kiely, Y. Zhang, T. Busch, and A. Ruschhaupt, EPJ Quantum Technol. **4**, 3 (2017).
[65] C. Whitty, A. Kiely, and A. Ruschhaupt, Phys. Rev. Res. **2**, 023360 (2020).
[66] G.-F. Wang, D.-F. Ye, L.-B. Fu, X.-Z. Chen, and J. Liu, Phys. Rev. A **74**, 033414 (2006).
[67] Y. Lahini, F. Pozzi, M. Sorel, R. Morandotti, D. N. Christodoulides, and Y. Silberberg, Phys. Rev. Lett. **101**, 193901 (2008).
[68] R. Menchon-Enrich, A. Benseny, V. Ahufinger, A. D. Greentree, T. Busch, and J. Mompart, Rep. Prog. Phys. **79**, 074401 (2016).
[69] H. Suchowski, G. Porat, and A. Arie, Laser Photon. Rev. **8**, 333 (2014).